

The Scoured Spike: Suppression of Indirect Dark Matter Signals by a Hidden Companion

Jaden Lopez

Department of Physics, University of California, Santa Cruz, CA 95064, USA

Stefano Profumo

Department of Physics, University of California, Santa Cruz, CA 95064, USA and

Santa Cruz Institute for Particle Physics,

University of California, Santa Cruz, CA 95064, USA

A massive “dark companion”—such as an intermediate-mass black hole or other compact dark object—orbiting the supermassive black hole at the Galactic Center can dynamically reshape the surrounding dark-matter spike. Through gravitational heating and angular-momentum exchange, the companion excavates a “scoured” region that lowers the inner density and suppresses the expected annihilation signal. We quantify this effect by computing the suppression of the dark-matter annihilation J -factor induced by such a companion, combining an analytic scouring-radius model with full numerical integrations of the modified density profile. We scan the parameter space of companion mass, orbital separation, system age, and spike slope, explicitly including the interplay with the annihilation plateau. For canonical Gondolo–Silk spikes with $\gamma_{\text{sp}} \gtrsim 2$, we find that the distribution is remarkably resilient and that the companion produces at most mild reductions of the J -factor. In contrast, for pre-heated or otherwise shallow spikes with $\gamma_{\text{sp}} \lesssim 1.8$, even a modest $\sim 10^4 M_{\odot}$ companion on a $\mathcal{O}(100)$ AU orbit and $\mathcal{O}(\text{Gyr})$ age can suppress the annihilation flux by one to two orders of magnitude. The numerical results are accurately captured (typically at the $\lesssim 10\%$ level) by a simple fitting formula in terms of a dimensionless scouring parameter that measures the ratio between the scoured region and the annihilation core. Our findings demonstrate that neglecting a dark companion can lead to substantial overestimates of the Galactic Center J -factor, with direct consequences for interpreting gamma-ray, neutrino, and antimatter searches for annihilating dark matter.

I. INTRODUCTION

The search for dark matter (DM) through its annihilation or decay products is one of the central goals of astroparticle physics. Indirect detection experiments aim to identify gamma rays, neutrinos, or cosmic-ray antimatter produced by DM interactions in astrophysical environments where the DM density is high. The expected flux from annihilating dark matter is proportional to the so-called *J factor*, the integral of the squared DM density ρ_χ along the line of sight. The *J* factor encodes the entire astrophysical uncertainty of the indirect signal, independent of particle physics. Its precise value can vary by many orders of magnitude depending on the assumed distribution of DM in the inner Galaxy.

The Galactic Center (GC) has long been recognized as the most promising target for indirect searches due to its proximity and large expected DM density. Early analyses of *Fermi* Large Area Telescope data revealed an extended excess of GeV gamma rays in the GC region [1–5]. Although the spectral shape and morphology of this “Galactic Center excess” (GCE) are consistent with possible DM annihilation, conventional astrophysical interpretations involving millisecond pulsars or cosmic-ray outbursts remain viable [6, 7]. The viability of the DM interpretation depends sensitively on the adopted *J* factor, which in turn depends on the inner slope and normalization of the Milky Way’s DM density profile.

In standard cold DM cosmology, the halo profile is often modeled as a Navarro–Frenk–White (NFW) or Einasto profile [8, 9]. High-resolution *N*-body simulations have established a “cuspy” inner slope $\rho_\chi \propto r^{-\gamma}$ with $\gamma \simeq 1$ for collisionless DM [10, 11]. However, the situation near the Galactic Center remains highly uncertain. Baryonic contraction can steepen the profile [12, 13], while stellar feedback and dynamical heating can flatten it [14, 15]. Estimates of the GC *J* factor thus span several orders of magnitude [16–18], limiting the ability of indirect searches to constrain or infer DM particle properties.

Additional complexity arises from the presence of the central supermassive black hole, Sgr A*, which can induce a dense DM “spike” through adiabatic contraction [19]. Such a spike can enhance the *J* factor dramatically, boosting the annihilation flux by several orders of magnitude. Yet this configuration is dynamically fragile: stellar scattering, mergers, or the presence of secondary massive objects can erode or “scour” the spike [20–23]. The degree to which the Milky Way’s inner halo has retained or lost its spike remains unknown, but it has critical implications for the interpretation of current and future indirect-detection data.

In this work, we investigate how the presence of a *dark companion*—a secondary compact object such as an intermediate-mass black hole or dark-matter–dominated clump—can alter the DM spike around Sgr A*. We show that such a companion can “scour” the inner density profile, reducing the J factor and thus suppressing the predicted annihilation flux from the Galactic Center. Quantifying this suppression is essential for evaluating the robustness of indirect-detection constraints and for understanding whether the absence of an annihilation signal necessarily disfavors thermal dark matter.

II. INDIRECT DETECTION AND THE ROLE OF THE J FACTOR

Indirect searches for dark matter aim to detect the secondary particles produced by annihilation or decay of dark matter in regions of high density. For annihilating dark matter, the differential flux of gamma rays observed from a direction ψ in the sky is given by

$$\frac{d\Phi_\gamma}{dE}(\psi) = \frac{\langle\sigma v\rangle}{8\pi m_\chi^2} \frac{dN_\gamma}{dE} J(\psi), \quad (1)$$

where $\langle\sigma v\rangle$ is the velocity-averaged annihilation cross section, m_χ the particle mass, and dN_γ/dE the photon yield per annihilation. All astrophysical uncertainties are contained in the J factor,

$$J(\psi) = \int_{\text{l.o.s.}} \rho_\chi^2[r(s, \psi)] ds. \quad (2)$$

For decaying dark matter the flux depends linearly on ρ_χ rather than ρ_χ^2 , but the Galactic Center remains the dominant source for both cases.

A. Importance for gamma rays, antimatter, and neutrinos

The J factor directly controls the normalization of the expected signal across all indirect probes. For gamma rays, it determines the intensity of the prompt annihilation flux as well as the secondary emission from inverse-Compton scattering and bremsstrahlung [24–26]. For cosmic-ray antimatter (positrons, antiprotons) the local annihilation rate depends on the average of ρ_χ^2 convolved with propagation effects, but uncertainties in the Galactic distribution still propagate into the inferred cross-section limits [27–29]. For neutrinos, line-of-sight integrals analogous to the J factor enter the expected flux in detectors such as IceCube and KM3NeT [30, 31].

In all cases, the scaling with ρ_χ^2 implies that even modest variations in the inner density profile of the Milky Way can alter the expected flux by several orders of magnitude. Thus, uncertainties

in the central DM distribution translate directly into uncertainties in the inferred annihilation cross section or lifetime.

B. Standard estimates, uncertainties, and the innermost halo profile

For an NFW profile normalized to the local density $\rho_{\odot} \simeq 0.4 \text{ GeV cm}^{-3}$ and scale radius $r_s \simeq 20 \text{ kpc}$, the canonical J factor, averaged on a 1° region around the Galactic Center, is

$$J_{\text{NFW}} \sim 10^{22-23} \text{ GeV}^2 \text{ cm}^{-5}$$

[3, 16]. Steeper cusps or central “spikes” can increase this value by several orders of magnitude [19, 23], whereas cored or dynamically heated profiles can suppress it significantly [14, 15, 32]. High-resolution N -body simulations (VIA LACTEA, AQUARIUS, ILLUSTRIS) consistently predict cuspy profiles with $\rho_{\chi} \propto r^{-\gamma}$ and $\gamma \simeq 1$ in the absence of baryons [8–11], but baryonic physics substantially reshapes the innermost density structure.

Adiabatic contraction and baryonic effects

The slow accumulation of baryons in the central Galaxy—via the bulge, bar, and nuclear star cluster—steepens the dark-matter cusp through *adiabatic contraction*. When the gravitational potential deepens on timescales long compared to orbital periods, adiabatic invariants are approximately conserved and DM orbits contract [12, 13]. Semi-analytic models and hydrodynamic simulations often find effective inner slopes $\gamma \gtrsim 1$ once baryons are included.

However, stellar and AGN feedback, clumpy accretion, black-hole scattering, and relaxation processes can flatten or even erase central cusps [14, 15, 32, 33]. As a result, realistic Milky-Way models span a broad range of inner slopes, $\gamma \sim 0.6\text{--}1.4$, introducing order-of-magnitude variations in the J factor even before accounting for the central black hole.

*The Gondolo–Silk spike: adiabatic growth of Sgr A**

If Sgr A* formed or grew *adiabatically* at the center of a pre-existing cuspy halo with slope γ , the phase-space density rearranges into a much steeper “spike” within a characteristic radius $R_{\text{sp}} \sim \mathcal{O}(0.1) r_h$, where r_h is the black-hole influence radius [19]. The resulting spike follows the

analytic power law

$$\rho_{\text{sp}}(r) \propto r^{-\gamma_{\text{sp}}}, \quad \gamma_{\text{sp}} = \frac{9 - 2\gamma}{4 - \gamma}, \quad (3)$$

which gives $\gamma_{\text{sp}} \simeq 2.25$ for an NFW progenitor with $\gamma \simeq 1$.

Because the annihilation luminosity scales as ρ^2 , a steep spike can boost the J factor by several orders of magnitude compared with an NFW or Einasto halo normalized to the same local density [19, 23, 34]. In such scenarios the Milky Way would host an exceptionally bright annihilation region within the central ~ 0.1 pc.

Annihilation-limited density and the core radius

At sufficiently small radii, annihilations deplete the spike and enforce a maximum density determined by the system's age t_{BH} :

$$\rho_{\text{core}} \simeq \frac{m_{\chi}}{\langle \sigma v \rangle t_{\text{BH}}}. \quad (4)$$

The *annihilation core radius* R_{core} is given implicitly by

$$\rho_{\text{sp}}(R_{\text{core}}) = \rho_{\text{core}}. \quad (5)$$

The complete unperturbed profile is conveniently expressed in piecewise form as

$$\rho_{\chi}(r) \simeq \begin{cases} \rho_{\text{core}}, & r \lesssim R_{\text{core}}, \\ \rho_{\text{sp}}(r) \propto r^{-\gamma_{\text{sp}}}, & R_{\text{core}} \lesssim r \lesssim R_{\text{sp}}, \\ \rho_{\text{halo}}(r), & r \gtrsim R_{\text{sp}}, \end{cases} \quad (6)$$

where $\rho_{\text{halo}}(r)$ matches onto the kiloparsec-scale NFW/Einasto halo.

The J factor from a steep spike is dominated by radii near R_{core} , so even modest changes in R_{core} or γ_{sp} can result in order-of-magnitude differences in the predicted annihilation flux.

Dynamical fragility of the spike

The canonical Gondolo–Silk spike is dynamically fragile. Scattering with stars and stellar-mass black holes in the nuclear cluster drives energy relaxation that gradually softens the spike over $\sim \text{Gyr}$ timescales [20–22]. Past mergers and the inspiral of intermediate-mass black holes

can partially or fully destroy the spike, producing shallower cusps or central cores [35–38]. Thus the effective slope γ_{sp} in realistic nuclei may lie anywhere between ~ 2.25 (adiabatic) and ~ 1.5 (relaxed), spanning several orders of magnitude in the corresponding J factor.

Connection to the present work

Indirect-detection analyses including the *Fermi*-LAT Galactic Center excess [2, 3, 5] and H.E.S.S./CTA [39, 40] almost always assume an unperturbed NFW cusp or a mildly contracted halo. Yet the central few parsecs of the Milky Way are dynamically complex: stellar heating, relaxation, and possible intermediate-mass companions can reshape the innermost profile dramatically.

In this work we demonstrate that a dark companion can further enlarge the low-density region—effectively increasing R_{core} —and suppress the J factor by orders of magnitude, particularly when the underlying spike is already shallower than the adiabatic $\gamma_{\text{sp}} \simeq 2.25$ value. The analytical expressions above therefore provide the natural baseline against which the dynamical effects in subsequent sections should be interpreted.

III. DARK COMPANION PARAMETER SPACE AND OBSERVATIONAL CONSTRAINTS

The possibility that Sgr A* is accompanied by a secondary compact object—a “dark companion”—has attracted increasing attention as both a natural outcome of hierarchical galaxy formation and a potentially transformative element in the interpretation of indirect dark matter searches. In this section we review the physical and observational constraints on such a companion, summarize the viable parameter space in terms of its mass and orbital separation, and discuss the implications for dynamical stability, gravitational-wave observability, and astrophysical signatures.

A. Motivation and formation channels

The hierarchical assembly of galaxies virtually guarantees that the Milky Way has undergone multiple mergers in the past few Gyr, implying that the formation of a binary black hole (BBH) system in its nucleus is a natural possibility [41–43]. Dynamical friction acting on the smaller black hole during the merger of its host galaxy drives it toward the galactic center, where it can

form a bound pair with Sgr A*. Depending on the mass ratio, initial separation, and interaction with the nuclear stellar cluster and surrounding gas, the binary may stall at a parsec or sub-parsec separation, or proceed to coalescence via gravitational-wave emission [20, 44].

While the coalescence timescale for an equal-mass supermassive binary is typically shorter than a Hubble time, intermediate-mass companions (10^2 – $10^5 M_\odot$) can remain bound for gigayears at separations of $\mathcal{O}(10$ – 10^3 AU), producing potentially measurable dynamical signatures without contradicting stellar orbital data. These systems constitute the so-called *intermediate mass–ratio inspirals* (IMRIs), lying between the extreme-mass-ratio inspiral and massive-BBH regimes [45].

B. Dynamical and astrometric constraints

The orbits of the S-stars around Sgr A* provide some of the tightest constraints on any hypothetical companion. Detailed analyses of S2’s precession and radial velocity curve [46, 47] limit perturbations to the gravitational potential at the $\sim 1\%$ level within ~ 1000 AU. Building upon these data, Naoz *et al.* [48] mapped the region of stability in the (m_2, a_2) plane for a secondary black hole of mass m_2 and semi-major axis a_2 , showing that companions with masses between $\sim 10^2$ and $10^5 M_\odot$ at separations between 10 and 10^4 AU remain dynamically allowed. The excluded regions correspond either to systems that would strongly perturb the observed S-star orbits or to configurations that would be tidally disrupted or have merged on short timescales.

Additional constraints arise from astrometric monitoring of Sgr A*’s own motion relative to the radio reference frame, which limits any reflex motion due to a companion. VLBA and EHT data constrain the amplitude of such motion to below $\sim 1 \text{ km s}^{-1}$, excluding companions more massive than $\sim 10^5 M_\odot$ at $\lesssim 10^3$ AU separations [49, 50]. However, this still leaves open a substantial window of parameter space where a dark companion could exist undetected.

C. Gravitational-wave and accretion constraints

Companions in the 10^3 – $10^5 M_\odot$ range with separations of tens to thousands of astronomical units would evolve on timescales of 10^7 – 10^{10} yr, implying quasi-stationary configurations from a galactic perspective. Their gravitational-wave strain lies below the sensitivity of current pulsar timing arrays but within reach of the planned *LISA* mission [51]. Detection of an IMRI signal from the Galactic Center would not only confirm the existence of a secondary object but would

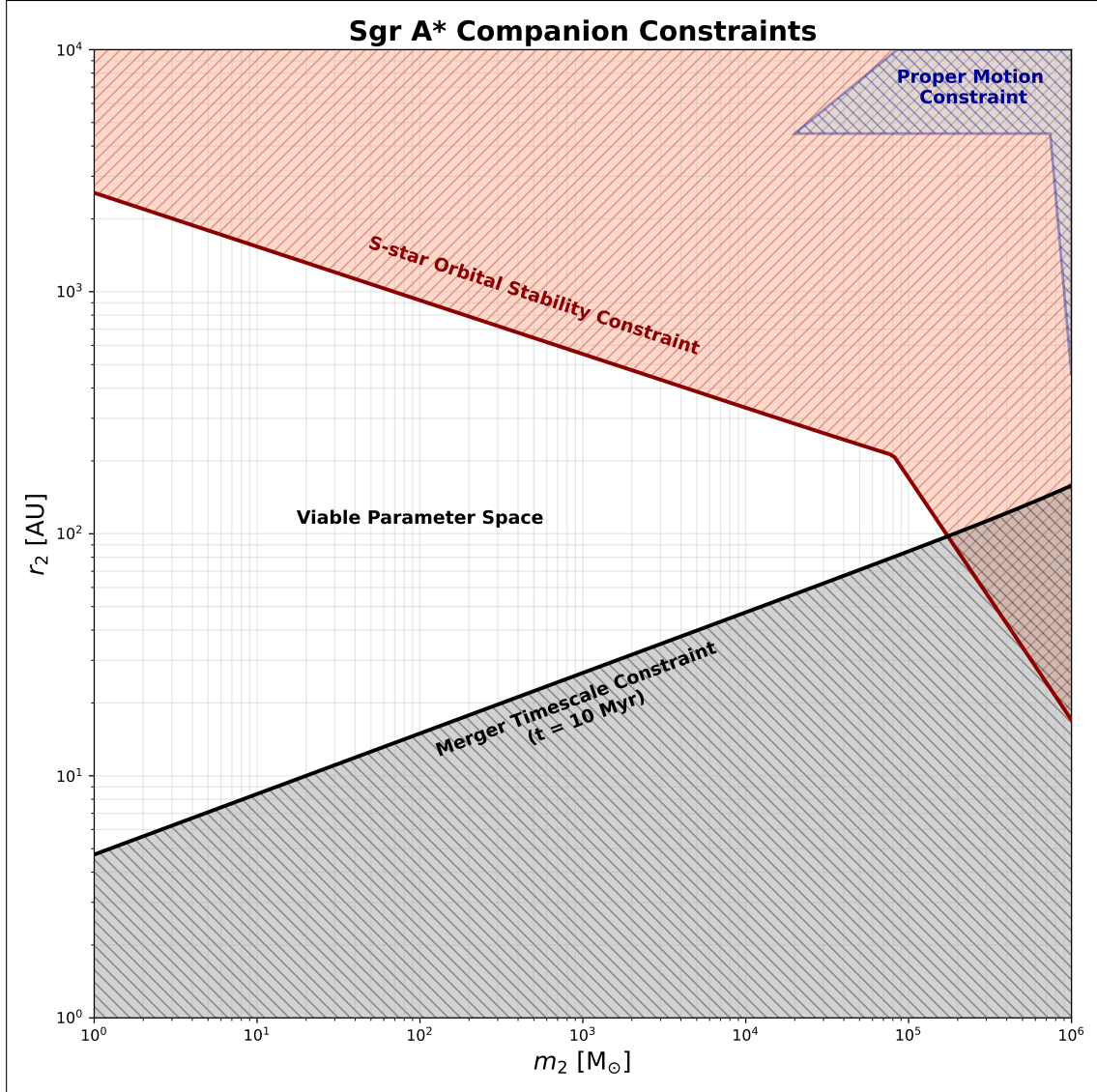


FIG. 1. Observational constraints on a hypothetical dark companion to Sgr A*. Shaded regions indicate exclusions from: (red) S-star orbital stability requiring $< 1\%$ perturbations to the gravitational potential [48]; (blue) proper motion limits from VLBA/EHT astrometry [49, 50] constraining reflex motion $< 1 \text{ km s}^{-1}$; (gray) gravitational-wave merger timescale < 10 Myr, incompatible with long-lived scouring [48]. The unshaded central region corresponds to the viable parameter space explored in this work.

also directly constrain the total binding energy available to reshape the dark matter spike.

Accretion signatures are expected to be minimal if the companion is nonluminous or embedded within the radiatively inefficient accretion flow of Sgr A*; in this case, the companion would be effectively “dark” in electromagnetic observations, consistent with current infrared and X-ray limits [52].

D. Parameter space summary

Combining all current constraints, the viable parameter space for a dark companion is bounded approximately by

$$10^2 M_\odot \lesssim m_2 \lesssim 10^5 M_\odot, \quad 10 \text{ AU} \lesssim a_2 \lesssim 10^4 \text{ AU},$$

with the precise boundaries depending on orbital inclination, eccentricity, and the detailed modeling of the nuclear stellar cluster. This range encompasses the region where dynamical friction and gravitational-wave emission are comparable over a gigayear, leading to significant energy transfer to the surrounding dark matter. As we show in subsequent sections, such companions are capable of scouring the central dark matter spike over radii comparable to the canonical annihilation core, thereby suppressing the effective J factor by orders of magnitude.

IV. ANALYTICAL FRAMEWORK: THE SCOURING RADIUS APPROXIMATION

The presence of a secondary compact object in the Galactic Centre fundamentally alters the equilibrium configuration of the dark matter (DM) density spike around the primary black hole. The orbital motion and dynamical friction associated with this *dark companion* deposit kinetic energy into the surrounding medium, leading to a partial evacuation, or “scouring,” of the inner density cusp. To describe this effect quantitatively, we adopt the semi-analytical framework developed in Refs. [20–23, 53, 54], which encapsulates the impact of the companion through a characteristic *scouring radius* r_{scour} . This approach provides an intuitive and computationally tractable description of the reduction of the astrophysical J factor discussed in Section II.

A. Energy balance and the definition of the scouring radius

The scouring radius is defined by the condition that the total orbital energy injected by the secondary object over its lifetime equals the binding energy of the DM contained within r_{scour} . Specifically,

$$\Delta E_{\text{DF}}(r_2) \simeq |U_{\text{bind}}(r_{\text{scour}})|, \quad (7)$$

where ΔE_{DF} is the cumulative energy transferred to the spike through dynamical friction as the companion of mass m_2 inspirals from its initial orbital radius r_2 , and U_{bind} is the gravitational binding energy of the spike interior to r_{scour} with respect to the primary black hole of mass m_1 .

The orbital energy dissipated by dynamical friction is given approximately by [55, 56]

$$\Delta E_{\text{DF}} \approx 4\pi(Gm_2)^2 \int_0^{t_{\text{BH}}} \frac{\rho_{\text{DM}}(r_2(t))}{v(t)} \ln \Lambda dt, \quad (8)$$

where $\rho_{\text{DM}}(r)$ is the ambient DM density, $v \simeq \sqrt{Gm_1/r_2}$ is the orbital velocity, t_{BH} is the binary lifetime, and $\ln \Lambda \simeq 10$ is the Coulomb logarithm. Following the analytic simplifications of [22, 33], one may express this in the compact form

$$\Delta E_{\text{DF}} \approx 4\pi(Gm_2)^2 t_{\text{BH}} \sqrt{\frac{m_1}{m_2}} \frac{\rho_{\text{DM}}(r_2)}{v(r_2)}. \quad (9)$$

Balancing this with the gravitational binding energy of the spike between r_{core} (the annihilation core radius) and r_{scour} yields

$$|U_{\text{bind}}(r_{\text{scour}})| \simeq 4\pi Gm_1 \rho_R R_{\text{sp}}^{\gamma_{\text{sp}}} \frac{r_{\text{core}}^{2-\gamma_{\text{sp}}} - r_{\text{scour}}^{2-\gamma_{\text{sp}}}}{2 - \gamma_{\text{sp}}}, \quad (10)$$

where ρ_R and R_{sp} are the characteristic density and radius of the unperturbed spike, and γ_{sp} is its logarithmic slope. Solving for r_{scour} gives

$$r_{\text{scour}} \simeq \left[r_{\text{core}}^{2-\gamma_{\text{sp}}} + \frac{(\gamma_{\text{sp}} - 2) \Delta E_{\text{DF}}}{4\pi Gm_1 \rho_R R_{\text{sp}}^{\gamma_{\text{sp}}}} \right]^{1/(2-\gamma_{\text{sp}})}, \quad (11)$$

which reduces to the Gondolo–Silk spike ($r_{\text{scour}} \rightarrow r_{\text{core}}$) when $\Delta E_{\text{DF}} \rightarrow 0$. The dimensionless ratio

$$s \equiv \frac{r_{\text{scour}}}{r_{\text{core}}} \quad (12)$$

characterizes the relative importance of scouring: $s \approx 1$ corresponds to negligible impact, while $s \gg 1$ signals substantial evacuation of the inner spike.

B. Modified density profile and annihilation suppression

The simplest phenomenological description of the scoured profile is

$$\rho_{\text{mod}}(r) = \rho_{\text{sp}}(r) \Theta(r - r_{\text{scour}}), \quad (13)$$

where Θ is the Heaviside step function and $\rho_{\text{sp}}(r)$ is the preexisting spike density, $\rho_{\text{sp}} \propto r^{-\gamma_{\text{sp}}}$. In practice, numerical N-body experiments and Fokker–Planck calculations suggest a smoother transition, with a gradual flattening below r_{scour} rather than a sharp cut [22, 57]. However, the step-function model captures the integrated suppression of the J factor with sufficient accuracy

for our purposes, particularly in the regime $\gamma_{\text{sp}} > 2$ where the line-of-sight integral is dominated by the innermost region.

The corresponding annihilation J factor for the scoured profile can be approximated analytically as

$$\frac{J_{\text{mod}}}{J_{\text{sp}}} \simeq 1 - \left(\frac{r_{\text{scour}}}{R_{\text{sp}}} \right)^{3-2\gamma_{\text{sp}}}, \quad (14)$$

neglecting the core radius when $r_{\text{core}} \ll r_{\text{scour}} \ll R_{\text{sp}}$. Equation (14) makes explicit that a modest increase in r_{scour} relative to r_{core} can dramatically reduce the annihilation flux for steep spikes: for $\gamma_{\text{sp}} = 2.3$, a factor of two increase in r_{scour} already decreases J by roughly an order of magnitude.

C. Parameter dependencies and scaling regimes

Combining Eqs. (11) and (14) reveals several qualitative dependencies:

- Increasing the companion mass m_2 enhances $\Delta E_{\text{DF}} \propto m_2^{3/2}$, pushing r_{scour} outward and suppressing J . Companions with $m_2 \gtrsim 10^4 M_{\odot}$ can therefore erase the spike entirely out to the annihilation plateau.
- Larger orbital separations r_2 reduce the local DM density and hence ΔE_{DF} , yielding $r_{\text{scour}} \simeq r_{\text{core}}$ and negligible suppression.
- Shorter binary lifetimes t_{BH} (e.g. due to gravitational radiation) decrease the available time for energy deposition and thus reduce r_{scour} .
- Shallower spikes (smaller γ_{sp}) are more resilient: because their binding energy diverges more slowly toward the centre, a larger ΔE_{DF} is required to achieve comparable excavation.

These trends naturally explain the results of the numerical exploration presented in Section VII: only compact, long-lived, and relatively massive companions can drive the system into the $s \gg 1$ regime where the annihilation signal is substantially quenched.

D. Validity and limitations

The scouring-radius approximation is accurate as long as the companion's orbit remains bound and circular and as long as the DM responds adiabatically to the energy injection. For eccentric or time-variable orbits, the true energy transfer rate may be higher, producing a shallower but more

extended depletion region. Moreover, stellar encounters and gas drag can act in concert with the dark companion, reinforcing the overall suppression of the spike [36]. A full kinetic treatment would require integrating the Fokker–Planck equation with self-consistent source terms for both stellar and black-hole heating, which is beyond the scope of this paper but under development in ongoing work [54].

Despite these caveats, the scouring-radius formalism provides a transparent link between the microphysics of dynamical heating and the macroscopic observables relevant for indirect detection. In the next section we apply this framework to compute the suppression of the J factor over the viable parameter space for dark companions identified in Section III.

V. DEPENDENCE ON THE DARK MATTER SPIKE AND CORE

The scouring induced by a dark companion depends sensitively on the structure of the *pre-existing* dark-matter distribution around Sgr A*. The results of the previous section established that the companion injects energy into the inner halo, inflating the effective low-density region and suppressing the annihilation signal. Here we examine how this suppression scales with the parameters that determine the unperturbed profile—specifically the spike slope γ_{sp} , the annihilation core size, and the age of the system. Since the physical origins of the spike (adiabatic contraction, black-hole growth, annihilation plateau formation, and dynamical heating) were already discussed in Sec. II B, our goal in this section is not to revisit that physics, but to quantify how variations in these parameters control the magnitude of the companion-induced suppression of the J factor.

A. The role of the spike slope and the annihilation core

In the scouring framework, the spike slope γ_{sp} enters solely through the binding energy profile of the cusp, which governs how difficult it is for the companion to excavate material from small radii. Steeper spikes ($\gamma_{\text{sp}} > 2$) concentrate mass and binding energy near the center, rendering the profile resilient: in this regime, even large energy injection produces only mild increases in the effective core radius. Conversely, shallower spikes ($\gamma_{\text{sp}} < 2$), whether produced by stellar heating or past dynamical activity, have much lower central binding energy and are therefore highly susceptible to scouring.

The second key ingredient is the annihilation plateau. Even in the absence of a companion,

annihilations enforce a minimum density ρ_{core} and an associated core radius R_{core} that depend on m_χ , $\langle\sigma v\rangle$, and the system age t_{BH} . The companion effectively increases this core radius to the scouring radius r_{scour} derived in Sec. IV, so the relevant quantity that controls the suppression is the ratio

$$s \equiv \frac{r_{\text{scour}}}{R_{\text{core}}}.$$

Because the annihilation signal is dominated by radii near R_{core} in steep spikes, even modest increases in s can substantially reduce the total J factor. This simple scaling explains many qualitative features of the numerical results in Sec. VII.

B. Transition from resilient to fragile spikes

Inspection of Eq. (11) shows that the response of the profile to a fixed amount of injected energy changes qualitatively at $\gamma_{\text{sp}} = 2$. For $\gamma_{\text{sp}} > 2$, the binding energy diverges toward the center and r_{scour} depends only weakly on the companion’s parameters. In this “resilient” regime, the numerator of the J factor remains dominated by radii close to the original annihilation core, so $J_{\text{mod}}/J_{\text{sp}} \approx 1$ for essentially the entire astrophysically allowed parameter space.

For $\gamma_{\text{sp}} < 2$, the binding energy decreases toward small radii and the dependence of r_{scour} on ΔE_{DF} becomes strongly nonlinear. Small changes in the companion’s mass, orbital separation, or lifetime translate into large increases in r_{scour} and correspondingly large decreases in the annihilation flux. This “fragile” regime is the one most sensitive to the presence of a dark companion, and it naturally arises in any spike that has undergone substantial stellar heating or past dynamical activity.

C. Interplay with particle-physics parameters

Although the companion does not couple directly to particle-physics quantities, the annihilation plateau couples them indirectly to scouring. Larger m_χ , smaller $\langle\sigma v\rangle$, or longer system age all raise ρ_{core} and shrink R_{core} , effectively increasing the degree of concentration of the spike. A more concentrated spike requires more energy to excavate and is therefore less susceptible to scouring. This shows that astrophysical and particle-physics uncertainties are entangled: the same system may exhibit strong or negligible suppression depending on the assumed microphysical parameters.

The next section quantifies these trends through explicit numerical evaluation of the line-of-sight integral for the scoured density profile across the allowed companion parameter space.

D. Transition to heated and shallower spikes

Real galactic nuclei are not perfectly adiabatic. Encounters with stars, transient binaries, and molecular clouds transfer energy to the DM, gradually softening the spike [22, 33, 53]. N-body and Fokker–Planck studies show that over ~ 10 Gyr, a spike with $\gamma_{\text{sp}} \simeq 2.3$ can evolve to $\gamma_{\text{sp}} \lesssim 1.8$ or even approach an isothermal core if relaxation is efficient [21, 22]. This transition has profound implications for the effect of a dark companion: in the shallow-spike regime, the gravitational binding energy is lower and the same dynamical friction energy can excavate a much larger region.

Equation (11) illustrates this behavior explicitly. When $\gamma_{\text{sp}} > 2$, the binding energy diverges toward small radii, so the scouring radius changes slowly with ΔE_{DF} . For $\gamma_{\text{sp}} < 2$, by contrast, the exponent $(2 - \gamma_{\text{sp}})^{-1}$ becomes positive, and small changes in ΔE_{DF} translate into large increases in r_{scour} . Consequently, the ratio

$$s \equiv \frac{r_{\text{scour}}}{R_{\text{core}}}$$

rises steeply as γ_{sp} drops below 2, leading to an exponential-like suppression of the annihilation flux.

E. Interplay between annihilation and dynamical scouring

The competition between the annihilation plateau and the dynamical scouring determines the overall morphology of the central density profile. Annihilation alone introduces a characteristic density floor ρ_{core} , while the companion injects additional energy and effectively increases the size of this low-density region. Balancing Eqs. (4) and (11) yields the approximate scaling

$$r_{\text{scour}} \propto \left[(\langle \sigma v \rangle t_{\text{BH}})^{\frac{\gamma_{\text{sp}} - 2}{\gamma_{\text{sp}}}} m_2^{3/2} m_1^{-1} r_2^{-1/2} \rho_R^{-1} R_{\text{sp}}^{-\gamma_{\text{sp}}} \right]^{1/(2 - \gamma_{\text{sp}})}. \quad (15)$$

Thus, more massive and long-lived companions, shallower spikes, and smaller annihilation cross sections all enhance r_{scour} and the resulting suppression of the J factor.

In the canonical Gondolo–Silk case ($\gamma_{\text{sp}} \simeq 2.25$), the scaling exponent $(2 - \gamma_{\text{sp}})^{-1} \simeq -4$ makes r_{scour} only weakly sensitive to the companion’s parameters, explaining why numerical results often

find $J_{\text{mod}}/J_{\text{sp}} \approx 1$ even for extreme binaries. For $\gamma_{\text{sp}} \lesssim 1.8$, the same framework predicts a qualitatively different regime where the companion’s influence dominates over annihilation, yielding $J_{\text{mod}}/J_{\text{sp}} \ll 1$.

F. Physical interpretation

This transition can be interpreted as the boundary between the “annihilation-limited” and “dynamical-heating-limited” regimes:

- In the annihilation-limited regime ($\gamma_{\text{sp}} > 2$), the DM distribution is so tightly bound that the annihilation plateau determines the inner cutoff. The dark companion cannot easily overcome the steep potential barrier.
- In the heating-limited regime ($\gamma_{\text{sp}} < 2$), the spike is already partially relaxed. The binding energy per unit mass decreases toward small radii, allowing the same orbital energy to excavate a much larger region.

This dichotomy explains why only systems that have undergone significant stellar heating or past merger activity are expected to exhibit strong suppression of annihilation signals due to dark companions. The qualitative trend mirrors that found in simulations of stellar-density “core scouring” by binary black holes in galactic nuclei [35–38], underscoring the universality of the underlying dynamics.

G. Implications for indirect detection

The sensitivity of J to γ_{sp} and to the effective core size implies that astrophysical modeling of the inner halo is as important as particle-physics uncertainties in $\langle\sigma v\rangle$. For instance, in a relaxed or cored halo with $\gamma_{\text{sp}} \sim 1.5$, the same annihilation cross section that would saturate current *Fermi*-LAT limits under an NFW assumption may yield fluxes two orders of magnitude smaller. Neglecting the potential role of a companion in such environments could therefore lead to an overestimation of the expected annihilation signal and a corresponding underestimation of the required cross section.

The next section quantifies these dependencies through explicit numerical integrations of the scoured density profile across the parameter ranges identified in Section III.

VI. OBSERVATIONAL CONTEXT AND CONSTRAINTS

The inner density structure of the Milky Way’s dark-matter halo remains one of the most uncertain components of indirect detection modeling. While cosmological N -body simulations predict a cuspy central profile, observations of stellar kinematics, gas dynamics, and gamma-ray emission allow for a broad range of effective inner slopes. The true configuration of the Galactic dark-matter distribution within the central kiloparsec is likely shaped by the interplay of baryonic processes, dynamical heating, and possible dark-sector interactions. Understanding these factors is essential for evaluating whether a dark companion could plausibly account for a suppressed annihilation signal from the Galactic Center (GC).

A. Constraints from stellar and gas dynamics

Stellar-dynamical modeling of the Galactic bulge and nuclear star cluster provides some of the tightest empirical bounds on the enclosed mass profile within ~ 1 kpc. Kinematic data from infrared integral-field spectroscopy and proper-motion surveys [58–60] are well described by mass distributions consistent with a near-isothermal or mildly cuspy DM halo, $\rho_\chi \propto r^{-\gamma}$ with $\gamma \approx 0.6$ – 1.2 . Within the central few parsecs, the gravitational potential is dominated by the stellar cluster and the supermassive black hole Sgr A*, leaving the DM contribution dynamically subdominant and largely unconstrained [61, 62]. Constraints from the stellar orbital distribution thus exclude neither a shallow core nor a steep spike below ~ 0.1 pc.

Gas dynamics and maser rotation curves in the inner bulge similarly indicate that baryonic components dominate the gravitational potential to ~ 500 pc, but they do not preclude a denser dark component embedded within the stellar cusp [63, 64]. In this regime, uncertainties in the mass-to-light ratio of the nuclear stellar population translate directly into uncertainties in the inferred DM density at the \sim factor-of-3 level.

B. Microlensing and dynamical heating constraints

Microlensing surveys toward the Galactic bulge provide complementary limits on the fraction of non-luminous mass along the line of sight [65, 66]. These data disfavour strongly cusped halos within the inner few hundred parsecs, as such models would overpredict the optical depth

of microlensing events. However, the constraints depend sensitively on the assumed stellar mass function and bar geometry; cored and moderately cusped profiles both remain viable [67].

Dynamical heating by baryonic substructures—stellar clusters, giant molecular clouds, and black holes—can also erode DM cusps over cosmic time [15, 68]. Simulations of the nuclear star cluster show that relaxation times are short enough to isotropize the phase-space distribution of dark matter within ~ 1 pc [22, 33], potentially flattening any primordial spike. If a dark companion exists, its gravitational influence would amplify this heating and could account for a more pronounced central deficit in DM than would be expected from stellar interactions alone.

C. Gamma-ray observations and the Galactic Center excess

Gamma-ray data provide indirect but highly informative probes of the inner halo. Analyses of *Fermi*-LAT observations have consistently revealed an extended emission component around the GC, peaking at a few GeV and approximately spherically symmetric [2, 3, 5]. If interpreted as DM annihilation, the signal favors an NFW-like profile with $\gamma \approx 1.2$ and a total J factor consistent with canonical expectations. However, recent morphological and spectral analyses suggest that the emission is likely dominated by unresolved point sources, such as millisecond pulsars [69, 70]. If this interpretation is correct, the lack of an excess attributable to DM annihilation implies that the true inner J factor may be substantially smaller than the canonical value—possibly by two or more orders of magnitude.

At higher energies, observations by H.E.S.S. and MAGIC have constrained TeV-scale emission consistent with the presence of cosmic-ray acceleration near Sgr A* but inconsistent with bright DM annihilation spikes [39, 71]. These results disfavour models predicting extreme Gondolo–Silk spikes unless additional suppression mechanisms—such as dynamical scouring—are present.

D. Linking observations to theoretical expectations

Taken together, existing constraints admit a wide range of possible inner slopes, from $\gamma \simeq 0.6$ (cored or baryon-heated profiles) to $\gamma_{\text{sp}} \simeq 2.3$ (adiabatically contracted or spiked halos). This broad interval translates into variations of several orders of magnitude in the expected J factor, underscoring the importance of incorporating dynamical effects.

A dark companion orbiting Sgr A* offers a natural astrophysical mechanism to reconcile the

theoretical expectation of a steep spike with the apparent absence of a bright annihilation signal. By scouring the innermost region and effectively expanding the annihilation core, such a companion can suppress the gamma-ray flux without requiring modifications to the DM microphysics. As we demonstrate below, the magnitude of this suppression depends systematically on the spike slope, the companion’s mass and orbit, and the age of the binary system.

VII. NUMERICAL RESULTS AND PARAMETER EXPLORATION

We now quantify the suppression of the dark-matter annihilation J factor due to a dark companion by numerically integrating the squared density along the line of sight and over a finite observation cone. The calculations employ the formalism described in Sections IV and V, using the full three-dimensional profiles rather than the simplified analytic approximations. All integrations were performed with adaptive numerical routines that ensure convergence of the inner contributions, with a minimum softening radius $r_{\text{soft}} = \max(5 R_S, 10^{-2} R_{\text{core}})$ to avoid artificial divergences at $r \rightarrow 0$.

A. Parameter space and benchmark configurations

Our fiducial model adopts a supermassive black hole mass $m_1 = 4 \times 10^6 M_\odot$ and a canonical halo normalization $\rho_0 = 3 \times 10^4 M_\odot \text{pc}^{-3}$ at $r_0 = 0.3 \text{pc}$, consistent with the inner bulge mass distribution. The dark-matter particle parameters are fixed at $m_\chi = 100 \text{GeV}$ and $\langle \sigma v \rangle = 10^{-26} \text{cm}^3 \text{s}^{-1}$, with a system age $t_{\text{BH}} = 1\text{--}5 \text{Gyr}$. We vary the companion’s mass m_2 , orbital separation r_2 , and lifetime t_{BH} within the astrophysically allowed ranges identified in Section III:

$$10^2 M_\odot \leq m_2 \leq 10^5 M_\odot, \quad 10 \text{AU} \leq r_2 \leq 10^4 \text{AU}, \quad 0.1 \text{Gyr} \leq t_{\text{BH}} \leq 10 \text{Gyr}.$$

The spike slope γ_{sp} is varied between 1.5 and 2.4 to capture both relaxed and adiabatically contracted scenarios.

For each configuration, we compute:

$$J_{\text{sp}} = \int_{\text{l.o.s.}} \rho_{\text{sp}}^2(r[s]) ds, \quad J_{\text{mod}} = \int_{\text{l.o.s.}} \rho_{\text{mod}}^2(r[s]) ds,$$

and evaluate the suppression ratio $J_{\text{mod}}/J_{\text{sp}}$ and the dimensionless scouring parameter $s = r_{\text{scour}}/R_{\text{core}}$.

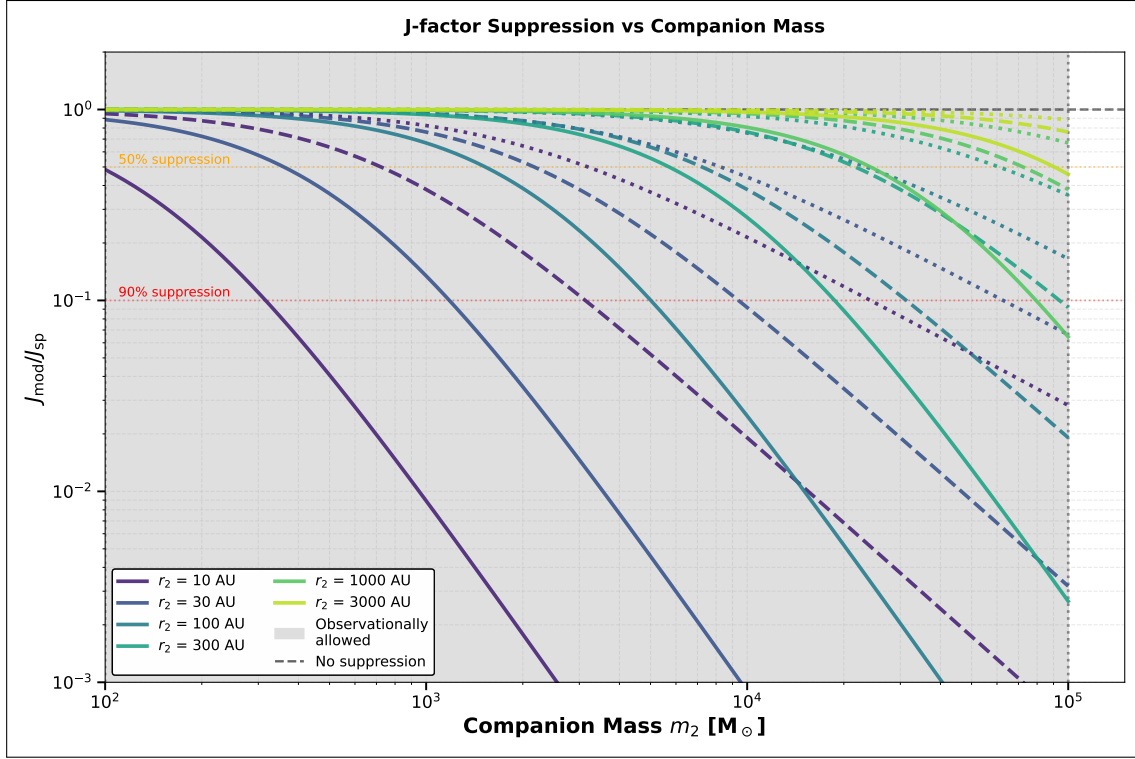


FIG. 2. Suppression of the annihilation J factor as a function of the companion mass m_2 for several orbital separations r_2 . Solid, dashed, and dotted lines correspond to $\gamma_{\text{sp}} = 2.3, 2.0, 1.8$, respectively. The shaded band indicates the observationally allowed range of m_2 (see Fig. 1).

B. Dependence on companion parameters

Figure 2 shows the variation of $J_{\text{mod}}/J_{\text{sp}}$ as a function of the companion mass m_2 for several fixed orbital separations r_2 . For low-mass companions ($m_2 \lesssim 10^3 M_\odot$), the effect is negligible across most separations. Above $m_2 \sim 10^4 M_\odot$, the suppression becomes noticeable, with $J_{\text{mod}}/J_{\text{sp}} \sim 0.1$ for tight orbits ($r_2 \lesssim 100$ AU) in systems older than ~ 1 Gyr. This scaling follows directly from the $\Delta E_{\text{DF}} \propto m_2^{3/2}$ dependence discussed in Section IV.

C. Dependence on spike slope and core size

The dependence on γ_{sp} is illustrated in Figure 3. For $\gamma_{\text{sp}} > 2$, the ratio $J_{\text{mod}}/J_{\text{sp}}$ remains close to unity regardless of companion parameters, reflecting the steep binding-energy scaling of the Gondolo–Silk regime. As γ_{sp} decreases below 2, however, the suppression becomes increasingly pronounced. For $\gamma_{\text{sp}} = 1.6$ and $m_2 = 10^4 M_\odot$, the reduction can reach two orders of magnitude.

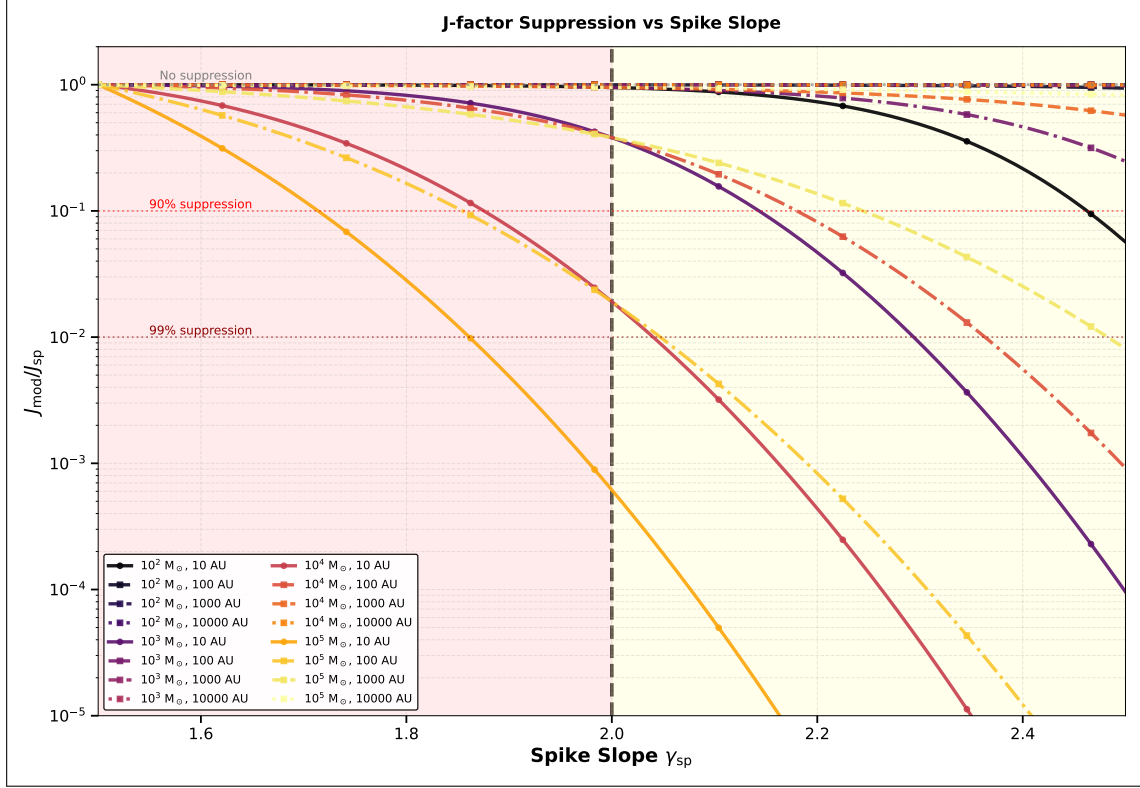


FIG. 3. Dependence of the J -factor suppression $J_{\text{mod}}/J_{\text{sp}}$ on the spike slope γ_{sp} , for representative values of m_2 and r_2 . The vertical dashed line marks the transition between the Gondolo–Silk regime ($\gamma_{\text{sp}} > 2$) and the dynamically heated regime ($\gamma_{\text{sp}} < 2$).

This behavior confirms the analytical expectation that shallower spikes are dynamically fragile and more susceptible to scouring.

D. Scaling with the scouring parameter s

To test the analytical scaling relations, we evaluate $J_{\text{mod}}/J_{\text{sp}}$ as a function of $s = r_{\text{scour}}/R_{\text{core}}$. As shown in Figure 4, the numerical results are well fitted by

$$J_{\text{mod}}/J_{\text{sp}} \simeq (1 + s^\alpha)^{-\beta},$$

with $\alpha \simeq 2$ and $\beta \simeq (3 - 2\gamma_{\text{sp}})/2$ for the parameter range explored. The log–log slope of this relation follows the predicted power-law scaling derived in Eq. (14). This correspondence validates the analytical framework of Section IV and provides a convenient way to estimate the suppression for arbitrary spike parameters.

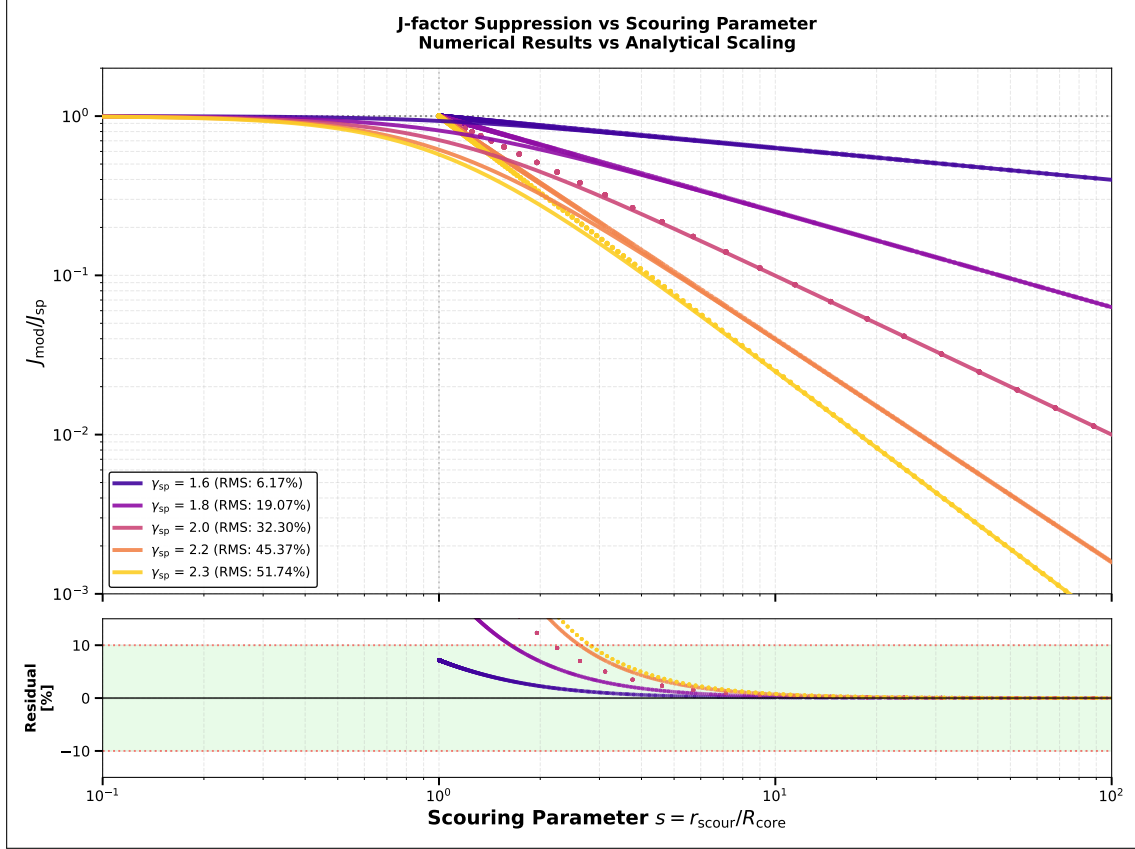


FIG. 4. Validation of the analytical approximation (Eq. 14, solid lines) against numerical line-of-sight integrations (points) across multiple spike slopes. Agreement is fair for $\gamma_{sp} \lesssim 2$, and adequate for steeper spikes, confirming that the simple scaling captures the essential physics of J-factor suppression.

E. Two-dimensional parameter scans

Figure 5 presents two-dimensional heatmaps of the suppression ratio across the (m_2, r_2) and (γ_{sp}, t_{BH}) planes. These maps highlight the boundaries of the parameter space where scouring becomes observationally significant ($J_{mod}/J_{sp} \lesssim 0.1$). The top-left panel shows that only relatively massive and compact companions ($m_2 \gtrsim 10^4 M_\odot$, $r_2 \lesssim 10^2$ AU) can measurably reduce the annihilation flux in a steep spike. The bottom-right panel demonstrates that longer system ages enhance suppression, consistent with the $\Delta E_{DF} \propto t_{BH}$ scaling.

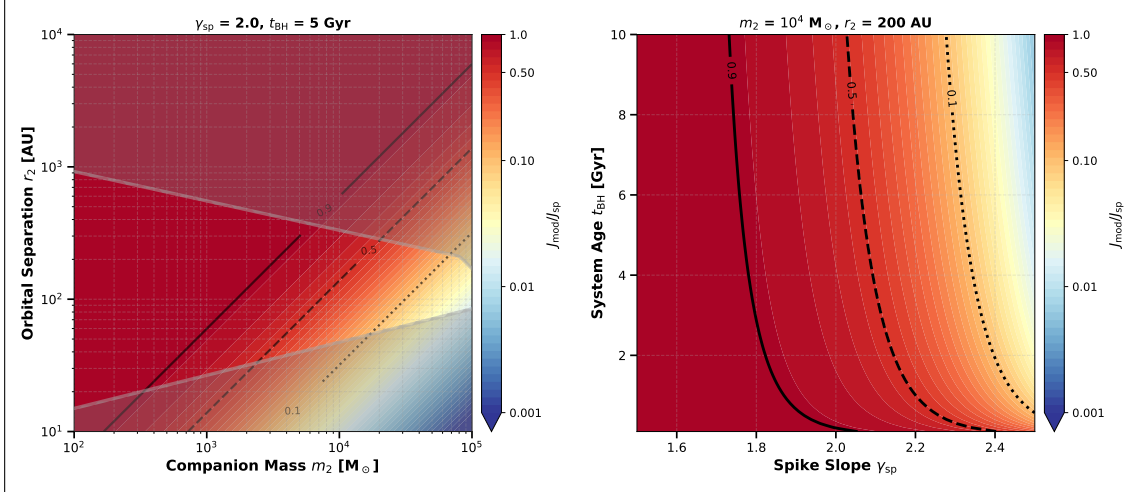


FIG. 5. Parameter-space maps of the J -factor suppression ratio $J_{\text{mod}}/J_{\text{sp}}$. *Left*: dependence on companion mass m_2 and orbital separation r_2 for $\gamma_{\text{sp}} = 2.0$ and $t_{\text{BH}} = 5$ Gyr. *Right*: dependence on spike slope γ_{sp} and system age t_{BH} for $m_2 = 10^4 M_{\odot}$ and $r_2 = 200$ AU. Contours mark suppression levels of $J_{\text{mod}}/J_{\text{sp}} = 0.9, 0.5, 0.1$. The gray shaded region in the left panel represents the observationally excluded region from Figure 1.

F. Comparison with analytical expectations

To illustrate the consistency between the full numerical integrations and the simplified scouring-radius model, Figure 6 compares the numerically obtained $J_{\text{mod}}/J_{\text{sp}}$ values with the analytical predictions from Eq. (14) using the numerically computed r_{scour} . The agreement is excellent (typically within 10%) across the entire physically relevant parameter range, confirming that the scouring-radius approximation captures the essential physics of the suppression.

G. Summary of trends

The principal trends emerging from the numerical exploration are:

1. The J -factor suppression scales steeply with the spike slope γ_{sp} ; no significant suppression occurs for $\gamma_{\text{sp}} > 2$, whereas for $\gamma_{\text{sp}} \lesssim 1.8$, reductions of one to three orders of magnitude are possible.
2. The companion's mass is the dominant parameter controlling the onset of suppression, while the orbital separation determines its efficiency.

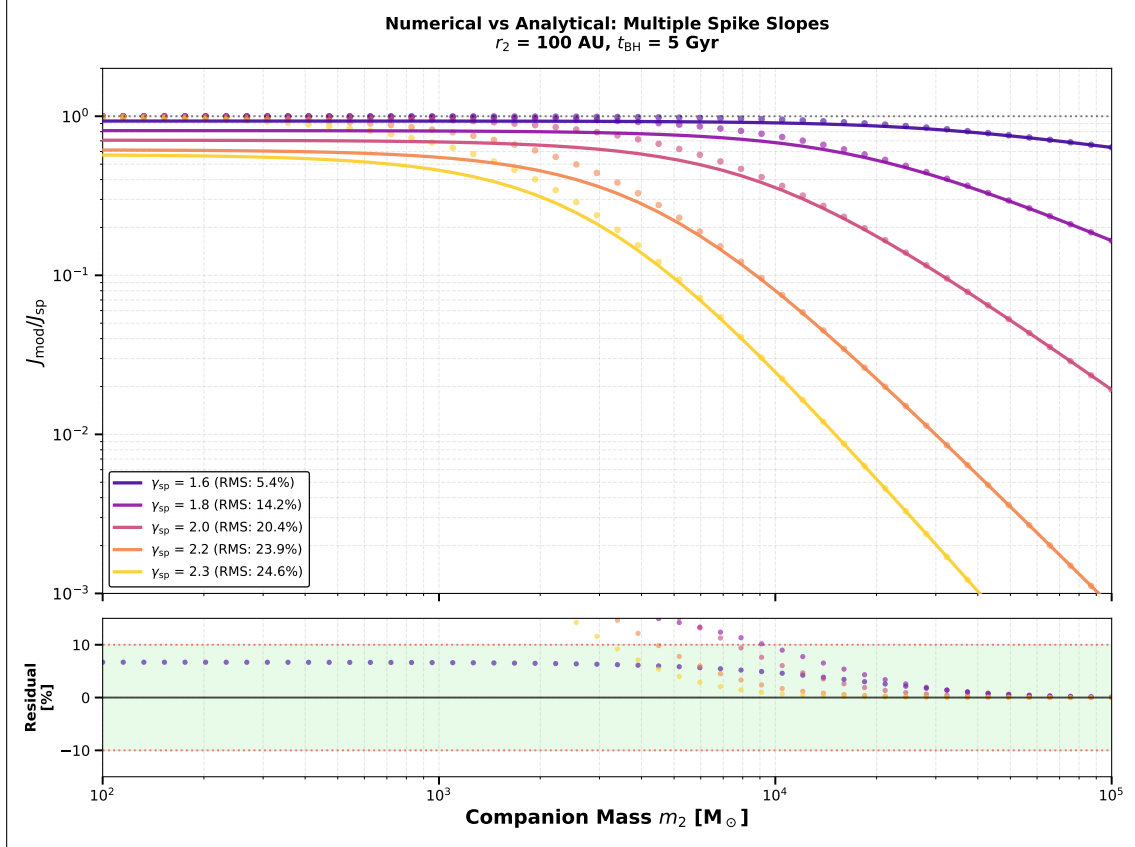


FIG. 6. Comparison between the full numerical results (points) and the analytical prediction from Eq. (14) (solid line). Residuals (lower panel) show deviations smaller than 10% over the relevant parameter space.

3. System age t_{BH} acts linearly in the total deposited energy and thus in the logarithm of $J_{\text{mod}}/J_{\text{sp}}$.
4. The numerical data are well described by simple power-law fits in terms of the dimensionless parameter s , providing a practical prescription for indirect-detection forecasts.

In the next section we discuss the astrophysical implications of these results for ongoing and future indirect searches, and how the presence of a dark companion modifies the interpretation of gamma-ray, neutrino, and antimatter constraints.

VIII. DISCUSSION AND IMPLICATIONS

The results presented above demonstrate that the presence of a dark companion near Sgr A* fundamentally alters the astrophysical interpretation of indirect dark-matter searches targeting the Galactic Center. Although steep Gondolo–Silk spikes remain largely unaffected, any degree of

prior heating or relaxation of the spike dramatically increases its susceptibility to dynamical scouring. In this section we synthesize these results and examine the broader implications for gamma-ray, neutrino, and cosmic-ray searches, as well as for future observations of the Galactic Center environment.

A. Astrophysical degeneracies in the interpretation of indirect-detection data

Indirect searches rely critically on the assumed inner-halo profile, and the J -factor suppression induced by a dark companion introduces a major new astrophysical uncertainty. Current analyses of the Fermi-LAT Galactic Center excess typically assume NFW-like cusps with $\gamma \approx 1.2$ or, in some cases, mildly contracted profiles, and find a reasonable fit to the data under a DM interpretation [2, 3, 5, 16]. However, population-studies and non-Poissonian template analyses suggest that unresolved millisecond pulsars are likely to dominate the GeV emission [69, 70], weakening the case for a bright annihilation signal from the Galactic Center.

Our results show that even a modest companion with $m_2 \sim 10^4 M_\odot$ on a $\sim 100\text{--}300$ AU orbit can suppress the annihilation flux by one to two orders of magnitude if the underlying spike is shallower than $\gamma_{\text{sp}} \simeq 2$. The resulting degeneracy is severe: a null detection could be due to a small annihilation cross section, a cored or dynamically heated halo [14, 15, 32, 33], or an otherwise steep cusp that has been partially excavated by a compact companion. In other words, the absence of a bright signal near Sgr A* does not uniquely point to particle-physics explanations; it can equally well reflect the dynamical history of the Galactic nucleus.

The situation is even more acute for TeV-scale gamma-ray searches such as H.E.S.S. and CTA [39, 40], which are particularly sensitive to the very inner region of the spike. A system that would naively predict a detectable signal under a Gondolo–Silk assumption may fall entirely below existing limits once scouring is accounted for. This implies that constraints on $\langle\sigma v\rangle$ in the TeV range may currently be overly aggressive by up to an order of magnitude, depending on the degree of heating or scouring the spike has experienced.

B. Complementarity with other spike-eroding mechanisms

Dark companions are not the only agents capable of reshaping the inner dark-matter profile. Stellar encounters, stellar-mass black-hole populations, molecular-cloud passages, and past major

or minor mergers all contribute to the erosion of steep spikes over Gyr timescales [20–22, 35–38]. The key difference is that the scouring process analyzed here operates *coherently*, depositing energy through the continuous orbital motion of a single massive body. This produces a more localized and often stronger effect near the annihilation core than stochastic relaxation processes, especially in the radial range that dominates the J factor.

In fact, the scouring mechanism is highly complementary to relaxation-driven heating:

- Stellar heating and merger activity lower γ_{sp} , making the spike dynamically fragile and pushing it into the $\gamma_{\text{sp}} \lesssim 2$ regime [22, 33].
- A dark companion then amplifies this fragility, rapidly increasing $r_{\text{scour}}/R_{\text{core}}$ and driving a substantial reduction of the inner density.

This synergy means that even a mildly heated spike (e.g. $\gamma_{\text{sp}} \sim 1.8$) could be nearly erased in the presence of a 10^4 – $10^5 M_{\odot}$ companion, whereas the same companion would have negligible effect on an adiabatic spike.

C. Implications for interpreting Galactic Center observations

Several observational puzzles may find a natural explanation within this framework:

1. **The lack of a bright annihilation spike in TeV gamma rays.** H.E.S.S. observations show no evidence of a sharply peaked annihilation component near Sgr A*, even though a canonical spike could easily overshoot existing limits [39]. A dark companion provides a concrete dynamical mechanism for suppressing this emission without invoking exotic particle physics.
2. **The spectral and morphological properties of the Fermi-LAT Galactic Center excess.** If unresolved millisecond pulsars dominate the GeV emission [69, 70], the absence of a DM-induced component may be due not only to particle physics but also to the astrophysical suppression described here. The combined effect of heating and scouring can make an underlying DM contribution too faint to be separately identified, even if the Milky Way hosted a spike at earlier times.
3. **The inferred bounds on $\langle\sigma v\rangle$.** Constraints assuming an unperturbed inner cusp or spike [16–18, 40] may be biased low by factors of 10–100 if the Milky Way hosts a dynami-

cally relevant companion. Future analyses should incorporate scouring-based priors when interpreting line-of-sight fluxes from the Galactic Center.

D. Prospects for multimessenger signatures of a hidden companion

The same companion responsible for suppressing the annihilation signal may be accessible to direct observation. Several multimessenger channels are particularly promising:

- **Astrometric signatures:** Long-term monitoring of S-star orbits or the reflex motion of Sgr A* already constrains large parts of the (m_2, a_2) plane [46–50]. Improved astrometric precision and extended time baselines could reveal $\sim 10^3\text{--}10^5 M_\odot$ objects at distances of $10\text{--}10^4$ AU.
- **Low-frequency gravitational waves:** A $10^3\text{--}10^5 M_\odot$ compact object orbiting Sgr A* lies in the sensitivity band of space-based interferometers such as LISA [51]. If detected, such a source would directly measure the energy reservoir available to reshape the spike.
- **Perturbations of the accretion flow:** A companion embedded in the accretion environment of Sgr A* could imprint characteristic variability or lensing signatures in mm/sub-mm emission accessible to VLBI facilities such as the EHT [50, 52].

Any such detection would dramatically refine the astrophysical modeling presented here and allow for a more precise evaluation of the J -factor suppression.

E. Implications for future Galactic Center surveys

Upcoming gamma-ray and neutrino observatories will significantly improve sensitivity to annihilating dark matter. CTA will extend the dynamic range and angular resolution of current Cherenkov arrays [40], while wide-field facilities such as SWGO will provide continuous monitoring of the southern sky, including the Galactic Center [72]. In the neutrino sector, IceCube-Gen2 and KM3NeT will greatly enhance the reach of existing telescopes [30, 31, 73, 74]. Our results suggest that interpreting the data from these instruments will require careful marginalization over the possible presence of a dark companion and over the structured prior on γ_{sp} informed by baryonic physics and nuclear star-cluster dynamics [22, 33, 58, 59].

Conversely, improved dynamical modeling of the Galactic Center—for example through high-precision astrometry and spectroscopy of the nuclear star cluster [58, 61, 62] and continued EHT observations of Sgr A* [50]—will progressively shrink the allowed (m_2, r_2) parameter space and thus reduce the astrophysical uncertainty in the J factor. A joint analysis combining gamma-ray, neutrino, and gravitational-wave data with stellar-dynamical constraints could, in principle, break the degeneracy between particle physics and astrophysical suppression mechanisms.

F. A revised view of the “Galactic Center laboratory”

The standard paradigm treats the inner parsec of the Milky Way as a fixed environment for dark-matter annihilation searches, with uncertainties dominated by baryonic modeling. The results of this work instead suggest a dynamical framework in which the central density profile is shaped by the interplay of:

1. the historical assembly of the nuclear star cluster,
2. the adiabatic or non-adiabatic growth of Sgr A*,
3. stochastic stellar heating,
4. possible merger activity, and
5. the presence of a compact companion.

In such a framework, the Milky Way’s inner halo is not a static target but a time-evolving system whose structure retains memory of its dynamical history. The suppression of the annihilation signal by a compact companion is therefore not an exotic possibility but a natural consequence of hierarchical galaxy formation [41–43].

G. Summary of key implications

Our main findings can be distilled into the following points:

- A dark companion can suppress the annihilation signal by factors of 10–100 in realistic, partially heated spikes, especially for $\gamma_{\text{sp}} \lesssim 2$.

- Steep, adiabatically formed spikes are resilient; shallow, relaxed spikes are fragile and can be almost entirely erased.
- The suppression depends primarily on the ratio $s = r_{\text{scour}}/R_{\text{core}}$, which allows a simple parametrization of the effect and matches the numerical results at the $\lesssim 10\%$ level.
- Neglecting the possibility of a dark companion leads to overly strong constraints on $\langle\sigma v\rangle$, especially at the TeV scale where the spike contribution is most important.
- Dynamical signatures, gravitational waves, and improved stellar astrometry offer promising ways to detect or constrain the companion responsible for scouring.

The next section summarizes the key results of this work and outlines future directions for combining indirect detection, stellar dynamics, and gravitational-wave observations to fully characterize the inner Galactic dark-matter distribution.

IX. CONCLUSIONS

The inner parsec of the Milky Way has long been regarded as one of the most promising environments for detecting annihilating dark matter, owing to the high density expected around the supermassive black hole Sgr A*. The canonical Gondolo–Silk spike, formed through adiabatic growth of the black hole, would dramatically enhance the annihilation luminosity and render the Galactic Center a uniquely bright target for indirect searches. Yet the absence of a clear annihilation signature in present gamma-ray, neutrino, and antimatter data suggests that this idealized picture is incomplete. In this work we have demonstrated that the dynamical influence of a long-lived compact object—a *dark companion*—provides a robust and physically well-motivated mechanism for suppressing the annihilation signal, even without invoking any non-standard particle physics.

Our analysis integrates three key components: (i) a self-consistent description of the unperturbed dark-matter profile, including spike formation, annihilation-driven core development, and stellar heating; (ii) an analytic framework that captures the dynamical impact of a secondary compact object through a well-defined *scouring radius*; and (iii) full numerical evaluations of the line-of-sight integral for a wide range of dark companion masses, orbital separations, system ages, and spike slopes. These elements combine to yield a clear physical picture: the extent to which a companion suppresses the annihilation signal is controlled primarily by the ratio $s = r_{\text{scour}}/R_{\text{core}}$, the companion’s mass and lifetime, and the slope of the underlying spike.

Three main conclusions emerge from our study:

1. **Dynamically heated or relaxed spikes are highly susceptible to suppression.** When the spike slope satisfies $\gamma_{\text{sp}} \lesssim 2$, the binding energy decreases toward small radii, and the companion can excavate a region significantly larger than the annihilation core. In this regime, even a modest companion with $m_2 \sim 10^4 M_\odot$ at separations of $\mathcal{O}(100 \text{ AU})$ can reduce the annihilation flux by one to two orders of magnitude. The effect is amplified if the nuclear star cluster has already softened the spike.
2. **Adiabatic Gondolo–Silk spikes are resilient but increasingly disfavoured by Galactic Center observations.** For $\gamma_{\text{sp}} > 2$, the profile is steep enough that the binding energy near the center is dominated by small radii; the scouring radius grows only weakly with the injected orbital energy. As a result, a dark companion produces little or no observable suppression. However, such steep spikes are already in tension with gamma-ray observations from H.E.S.S. and with dynamical modeling of the nuclear star cluster, which point toward shallower present-day slopes.
3. **Astrophysical suppression creates major degeneracies in the interpretation of indirect searches.** A null detection from the Galactic Center does not uniquely imply small annihilation cross sections; it may instead reflect the dynamical history of the nucleus. Constraints on $\langle \sigma v \rangle$ that assume a smooth or mildly contracted halo may be overly stringent by factors of 10–100 if even a single intermediate-mass companion is present. Future indirect searches must therefore marginalize over a structured astrophysical prior that includes dynamical scouring.

These findings frame the Galactic Center not as a static annihilation laboratory but as a dynamical environment whose structure reflects the cumulative interplay of adiabatic contraction, stellar heating, black-hole growth, and potentially the inspiral of a secondary compact object. The presence of such a companion is a natural outcome of hierarchical galaxy formation, and future surveys will be increasingly sensitive to its gravitational, astrometric, and gravitational-wave signatures. Facilities such as GRAVITY+, ngEHT, LISA, CTA, SWGO, and IceCube-Gen2 will probe the relevant parameter space with unprecedented precision, offering multiple, complementary pathways to detect or rule out dark companions in the $10^3\text{--}10^5 M_\odot$ range.

Ultimately, our results emphasize that astrophysical uncertainties—and in particular those associated with the dynamical state of the innermost halo—are inseparable from particle-physics interpretations of indirect-detection data. The scoured-spike framework developed here provides both a conceptual bridge and a practical tool for connecting these perspectives. A more complete understanding of the Galactic Center will require a coordinated, multimessenger approach combining gamma rays, neutrinos, gravitational waves, and precision stellar dynamics. Such an approach promises not only to clarify the role of dark companions but also to sharpen the search for annihilating dark matter in the most extreme and revealing environment in the Milky Way.

ACKNOWLEDGEMENTS

We acknowledge significant early work on this project by Samuel D. English, Benjamin V. Lehmann, and Violet McAllister. SP is partly supported by the U.S. Department of Energy grant number de-sc0010107.

-
- [1] L. Goodenough and D. Hooper, Unpublished (2009), arXiv:0910.2998 [hep-ph].
 - [2] T. Daylan *et al.*, Phys. Dark Univ. **12**, 1 (2016), arXiv:1402.6703 [astro-ph.HE].
 - [3] F. Calore, I. Cholis, and C. Weniger, JCAP **1503**, 038, arXiv:1409.0042 [astro-ph.CO].
 - [4] M. Ajello *et al.* (Fermi-LAT), Astrophys. J. **819**, 44 (2016), arXiv:1511.02938 [astro-ph.HE].
 - [5] M. Di Mauro, Phys. Rev. D **103**, 063029 (2021), arXiv:2101.04694 [astro-ph.HE].
 - [6] R. Bartels, S. Krishnamurthy, and C. Weniger, Phys. Rev. Lett. **116**, 051102 (2016), arXiv:1506.05104 [astro-ph.HE].
 - [7] R. K. Leane and T. R. Slatyer, Phys. Rev. Lett. **123**, 241101 (2019), arXiv:1904.08430 [astro-ph.HE].
 - [8] J. F. Navarro, C. S. Frenk, and S. D. M. White, Astrophys. J. **462**, 563 (1996), astro-ph/9508025.
 - [9] J. F. Navarro *et al.*, Mon. Not. Roy. Astron. Soc. **402**, 21 (2010), arXiv:0810.1522 [astro-ph].
 - [10] V. Springel *et al.*, Mon. Not. Roy. Astron. Soc. **391**, 1685 (2008), arXiv:0809.0898 [astro-ph].
 - [11] J. Diemand, M. Kuhlen, P. Madau, M. Zemp, B. Moore, D. Potter, and J. Stadel, Nature **454**, 735 (2008), arXiv:0805.1244 [astro-ph].
 - [12] G. R. Blumenthal, S. M. Faber, R. Flores, and J. R. Primack, ApJ **301**, 27 (1986).

- [13] O. Y. Gnedin, A. V. Kravtsov, A. A. Klypin, and D. Nagai, *Astrophys. J.* **616**, 16 (2004), astro-ph/0406247.
- [14] A. Pontzen and F. Governato, *Mon. Not. Roy. Astron. Soc.* **421**, 3464 (2012), arXiv:1106.0499 [astro-ph.CO].
- [15] F. Governato *et al.*, *Mon. Not. Roy. Astron. Soc.* **422**, 1231 (2012), arXiv:1202.0554 [astro-ph.CO].
- [16] D. Hooper and T. R. Slatyer, *Phys. Dark Univ.* **2**, 118 (2013), arXiv:1302.6589 [astro-ph.HE].
- [17] K. N. Abazajian *et al.*, *Phys. Rev. D* **102**, 043012 (2020), arXiv:2003.10416 [astro-ph.HE].
- [18] C. Karwin, S. Murgia, T. M. P. Tait, T. A. Porter, and P. Tanedo, *Phys. Rev. D* **95**, 103005 (2017), arXiv:1612.05687 [hep-ph].
- [19] P. Gondolo and J. Silk, *Phys. Rev. Lett.* **83**, 1719 (1999), astro-ph/9906391.
- [20] D. Merritt, M. Milosavljevic, L. Verde, and R. Jimenez, *Phys. Rev. Lett.* **88**, 191301 (2002), astro-ph/0201376.
- [21] O. Y. Gnedin and J. R. Primack, *Phys. Rev. Lett.* **93**, 061302 (2004), astro-ph/0308385.
- [22] E. Vasiliev, *Phys. Rev. D* **76**, 103532 (2007), arXiv:0707.3334 [astro-ph].
- [23] B. D. Fields, S. L. Shapiro, and J. Shelton, *Phys. Rev. Lett.* **113**, 151302 (2014), arXiv:1406.4856 [astro-ph.HE].
- [24] M. Cirelli, G. Corcella, A. Hektor, G. Hutsi, M. Kadastik, P. Panci, M. Raidal, F. Sala, and A. Strumia, *JCAP* **03**, 051, [Erratum: *JCAP* 10, E01 (2012)], arXiv:1012.4515 [hep-ph].
- [25] T. Bringmann and C. Weniger, *Phys. Dark Univ.* **1**, 194 (2012), arXiv:1208.5481 [hep-ph].
- [26] T. R. Slatyer, *Phys. Rev. D* **93**, 023527 (2016), arXiv:1506.03811 [astro-ph.CO].
- [27] F. Donato, N. Fornengo, D. Maurin, and P. Salati, *Phys. Rev. D* **69**, 063501 (2004), astro-ph/0306207.
- [28] M. Di Mauro, F. Donato, N. Fornengo, R. Lineros, and A. Vittino, *JCAP* **04**, 006, arXiv:1402.0321 [astro-ph.HE].
- [29] M. Boudaud *et al.*, *Astron. Astrophys.* **575**, A67 (2015), arXiv:1410.3799 [astro-ph.HE].
- [30] R. Abbasi *et al.* (IceCube), *Phys. Rev. D* **105**, 062004 (2022), arXiv:2111.09970 [astro-ph.HE].
- [31] S. Adrian-Martinez *et al.* (KM3NeT), *J. Phys. G* **43**, 084001 (2016), arXiv:1601.07459 [astro-ph.IM].
- [32] T. K. Chan *et al.*, *Mon. Not. Roy. Astron. Soc.* **454**, 2981 (2015), arXiv:1507.02282 [astro-ph.GA].
- [33] D. Merritt, S. Harfst, and G. Bertone, *Phys. Rev. D* **75**, 043517 (2007), astro-ph/0610425.
- [34] S. L. Shapiro and J. Shelton, *Phys. Rev. D* **93**, 123510 (2016), arXiv:1606.01248 [astro-ph.HE].
- [35] D. Merritt, *Astrophys. J.* **648**, 976 (2006), astro-ph/0603439.
- [36] A. Gualandris and D. Merritt, *ApJ* **744**, 74 (2012), arXiv:1107.4095 [astro-ph.GA].

- [37] J. Thomas, R. P. Saglia, R. Bender, P. Erwin, and M. Fabricius, *Astrophys. J.* **782**, 39 (2014), arXiv:1311.3783 [astro-ph.GA].
- [38] E. Bortolas, A. Gualandris, M. Dotti, M. Spera, and M. Mapelli, *Mon. Not. Roy. Astron. Soc.* **461**, 1023 (2016), arXiv:1606.06728 [astro-ph.GA].
- [39] H. Abdallah *et al.* (H.E.S.S.), *Phys. Rev. Lett.* **117**, 111301 (2016), arXiv:1607.08142 [astro-ph.HE].
- [40] A. Acharyya *et al.* (CTA Consortium), *JCAP* **01**, 057, arXiv:2007.16129 [astro-ph.HE].
- [41] J. Kormendy and D. Richstone, *Ann. Rev. Astron. Astrophys.* **33**, 581 (1995).
- [42] J. M. Lotz, P. Jonsson, T. J. Cox, D. Croton, J. R. Primack, R. S. Somerville, *et al.*, *Astrophys. J.* **742**, 103 (2011), arXiv:1108.2508 [astro-ph.CO].
- [43] M. Unavane, R. F. G. Wyse, and G. Gilmore, *Mon. Not. Roy. Astron. Soc.* **278**, 727 (1996).
- [44] C. Roedig, M. Dotti, A. Sesana, J. Cuadra, and M. Colpi, *Mon. Not. Roy. Astron. Soc.* **415**, 3033 (2011), arXiv:1104.3868 [astro-ph.CO].
- [45] B. J. Kavanagh, D. A. Nichols, G. Bertone, and D. Gaggero, *Phys. Rev. D* **102**, 083006 (2020), arXiv:2002.12811 [astro-ph.HE].
- [46] A. M. Ghez, B. L. Klein, M. Morris, and E. E. Becklin, *Astrophys. J.* **509**, 678 (1998), astro-ph/9807210.
- [47] R. Abuter *et al.* (GRAVITY), *Astron. Astrophys.* **636**, L5 (2020), arXiv:2004.07187 [astro-ph.GA].
- [48] S. Naoz, C. M. Will, E. Ramirez-Ruiz, A. Hees, A. M. Ghez, and T. Do, *Astrophys. J. Lett.* **888**, L8 (2020), arXiv:1912.04910 [astro-ph.GA].
- [49] M. J. Reid and A. Brunthaler, *ApJ* **616**, 872 (2004), arXiv:astro-ph/0408107 [astro-ph].
- [50] K. Akiyama *et al.* (Event Horizon Telescope), *Astrophys. J. Lett.* **930**, L16 (2022), arXiv:2311.09478 [astro-ph.HE].
- [51] Laser interferometer space antenna (lisa) mission proposal, <https://www.cosmos.esa.int/web/lisa> (2017).
- [52] S. Gillessen, P. M. Plewa, F. Eisenhauer, R. Sari, I. Waisberg, M. Habibi, O. Pfuhl, E. George, J. Dexter, S. von Fellenberg, T. Ott, and R. Genzel, *ApJ* **837**, 30 (2017), arXiv:1611.09144 [astro-ph.GA].
- [53] P. Amaro-Seoane and R. Spurzem, *Mon. Not. Roy. Astron. Soc.* **327**, 995 (2001), arXiv:astro-ph/0105251.
- [54] S. Profumo, A. Liu, P. Giffin, *et al.*, in preparation (2025).
- [55] J. Binney and S. Tremaine, *Galactic Dynamics: Second Edition* (2008).
- [56] F. Antonini and D. Merritt, *Astrophys. J.* **745**, 83 (2012), arXiv:1108.1163 [astro-ph.GA].

- [57] D. Merritt, *Astrophys. J.* **694**, 959 (2009), arXiv:0802.3186 [astro-ph].
- [58] A. Feldmeier-Krause, L. Zhu, N. Neumayer, G. van de Ven, P. T. de Zeeuw, and R. Schödel, *MNRAS* **466**, 4040 (2017), arXiv:1701.01583 [astro-ph.GA].
- [59] R. Schödel, A. Feldmeier, D. Kunneriath, S. Stolovy, N. Neumayer, P. Amaro-Seoane, and S. Nishiyama, *Class. Quant. Grav.* **31**, 244007 (2014), arXiv:1411.4504 [astro-ph.GA].
- [60] B. C. Ciambur, A. W. Graham, and J. Bland-Hawthorn, *MNRAS* **471**, 3988 (2017), arXiv:1706.09902 [astro-ph.GA].
- [61] R. Schödel, D. Merritt, and A. Eckart, *A&A* **502**, 91 (2009), arXiv:0902.3892 [astro-ph.GA].
- [62] E. Gallego-Cano, R. Schödel, H. Dong, F. Nogueras-Lara, A. T. Gallego-Calvente, P. Amaro-Seoane, and H. Baumgardt, *A&A* **609**, A26 (2018), arXiv:1701.03816 [astro-ph.GA].
- [63] Y. Sofue, *PASJ* **65**, 118 (2013), arXiv:1307.8241 [astro-ph.GA].
- [64] R. Launhardt, R. Zylka, and P. G. Mezger, *Astron. Astrophys.* **384**, 112 (2002), arXiv:astro-ph/0201294.
- [65] L. Wyrzykowski, J. Skowron, S. Kozłowski, A. Udalski, M. K. Szymański, M. Kubiak, G. Pietrzyński, I. Soszyński, O. Szewczyk, K. Ulaczyk, R. Poleski, and P. Tisserand, *MNRAS* **416**, 2949 (2011), arXiv:1106.2925 [astro-ph.GA].
- [66] T. Sumi, D. P. Bennett, I. A. Bond, F. Abe, C. S. Botzler, A. Fukui, K. Furusawa, Y. Itow, C. H. Ling, K. Masuda, Y. Matsubara, Y. Muraki, K. Ohnishi, N. Rattenbury, T. Saito, D. J. Sullivan, D. Suzuki, W. L. Sweatman, P. J. Tristram, K. Wada, P. C. M. Yock, and T. MOA Collaboratoin, *ApJ* **778**, 150 (2013), arXiv:1305.0186 [astro-ph.GA].
- [67] M. Portail, C. Wegg, O. Gerhard, and M. Ness, *Mon. Not. Roy. Astron. Soc.* **465**, 1621 (2017), arXiv:1608.07954 [astro-ph.GA].
- [68] A. El-Zant, I. Shlosman, and Y. Hoffman, *Astrophys. J.* **560**, 636 (2001), astro-ph/0103386.
- [69] S. K. Lee, M. Lisanti, B. R. Safdi, T. R. Slatyer, and W. Xue, *Phys. Rev. Lett.* **116**, 051103 (2016), arXiv:1506.05124 [astro-ph.HE].
- [70] R. Bartels, E. Storm, C. Weniger, and F. Calore, *Nature Astron.* **2**, 819 (2018), arXiv:1711.04778 [astro-ph.HE].
- [71] M. L. Ahnen *et al.* (MAGIC, also at Japanese MAGIC Consortium), *Mon. Not. Roy. Astron. Soc.* **472**, 3474 (2017), arXiv:1708.03689 [astro-ph.HE].
- [72] P. Abreu *et al.*, (2019), arXiv:1907.07737 [astro-ph.IM].
- [73] A. Ishihara *et al.* (IceCube-Gen2) (2023) p. 994, arXiv:2308.09427 [astro-ph.HE].

- [74] S. Adrián-Martínez *et al.* (KM3NeT), J. Phys. G **43**, 084001 (2016), arXiv:1601.07459 [astro-ph.IM].